Theory of multicomponent wiggler free-electron lasers in the small-signal regime

Chun-Ching Shih and Maria Zales Caponi
TRW Energy Systems Operations, One Space Park, Redondo Beach, California 90278
(Received 14 September 1981; revised manuscript received 20 January 1982)

A theory of the multicomponent wiggler free-electron laser is formulated in the small-signal regime. Analytical expressions for the spontaneous spectrum and the corresponding small-signal gain are derived. The expressions are valid for an arbitrary wiggler configuration consisting of any number of constant or tapered sections and drift spaces. Thus, optical klystrons are included as a particular case of the two-component devices. As a natural result of the derivation, it is proved that Madey's theorem holds for any multicomponent wiggler configuration including the optical klystron. As particular cases, several two-component wiggler schemes are discussed in detail. Based on the simple-gain expression an upper limit is obtained for the small-signal gain. It is shown that this cannot exceed the maximum gain of a constant wiggler of the same effective length by more than 25%.

I. INTRODUCTION

The free-electron laser (FEL) is a device that utilizes the interaction of relativistic electrons and the radiation in a periodic magnetic field (wiggler) to generate coherent and tunable electromagnetic radiation. It is well known that a properly tapered wiggler can extract more electron energy than an untapered wiggler to amplify the input signal of a small output wavelength ($\lambda \lesssim 10$ μm) FEL at high powers ($\gtrsim 10$ MW).[1] The physical principle is based on keeping the phase velocity of the ponderomotive potential well, formed by the interaction wiggler field with the electrons and the radiation field, in pace with the electron mean velocity in such a way that the energy extraction process can be continued down the wiggler. This is accomplished by either spatially varying the phase velocity of the potential (well) bucket or by replenishing the longitudinal energy lost by the electron beam to radiation. The phase velocity can be varied in a controlled manner by adiabatically tapering the wiggler period whereas the longitudinal electron energy can be replenished by either adiabatically tapering the wiggler amplitude or introducing a dc longitudinal electric field. The electrons that are initially trapped in the bucket tend to remain trapped if the motion is sufficiently adiabatic. As the bucket energy or its amplitude decreases, the mean energy of the trapped electrons is reduced. The extracted electron beam energy provides the amplification of the input laser signal.

The appropriate taper of the wiggler depends on the rate of change of the electron beam energy which is, in turn, strongly related to the radiation field strength. Therefore, a wiggler with a given taper is optimum only for certain input laser power level. The single-pass gain decreases for either higher or lower input power. At low input powers (small signal), the gain can drop to a much lower value than at high powers. Further, for low input powers, the gain can become negative for those frequencies that are optimum at high powers. This could present serious problems for the startup of a free-electron laser oscillator.

If the oscillator is started by injecting a low power signal at the desired wavelength, the system will be practical only if the injected power is less, at least, than one-tenth of the optimum power. Usually, this power level is well within the small-signal regime. If the roundtrip cavity loss, including the output coupling, is larger than the single-pass gain, the oscillator can never start. The characteristics of the tapered wiggler FEL at optical frequencies are such that even in cases where the small-signal gain is higher than the threshold value, the net gain is usually too small for the radiation field to reach its saturation within a finite number of passes (typically, for a high currect rf linac accelerator, there are only several hundred micropulses in an electron macropulse). The problem may be alleviated by utilizing storage rings, superconducting linacs, or other electron sources that are essentially cw systems. With the present state of the art, however, these accelerators cannot support the extremely high currents ($I > 50$ A) that are necessary to obtain gain

above threshold for the small wavelengths and high powers of interest. Recently, it has been suggested that the small-signal gain, as well as the large-signal gain, could be enhanced by utilizing multicomponent devices[2–4] or optical klystrons.[5,6]

If the oscillator is started from the noise level, it will oscillate at the wavelength where the gain is maximum. The maximum energy extraction occurs when there is maximum overlap in the interaction region between the electron mean velocity and the bucket phase velocity (resonant). However, at small signals, the electron energy loss is slower than the rate for which the tapered wiggler is designed. Thus, to obtain higher gain at small-signal levels the starting electron energy would have to be lower than the resonant energy. For fixed electron energy, this means that the wavelength at which the maximum gain occurs varies with the input power. This effect can produce a shift of the operating radiation wavelength as the radiation builds up inside the cavity.[7] In addition, it also suggests that injected oscillators should be started with a signal at the maximum gain wavelength instead of the final, desired wavelength. Although this might solve the start-up problem, it can delay the time to reach steady state beyond acceptable limits. The adiabatic condition for the shift and how it proceeds at the expense of the interaction gain need to be studied carefully.

In order to analyze these two aspects of a tapered wiggler FEL oscillator, we undertook the study of the more fundamental problem that is reported in this paper: the analysis of the small-signal gain spectrum which determines the gain magnitude as well as the operating wavelength. The result from these studies motivated a full investigation of the novel multicomponent wiggler scheme.[3] The analysis of this scheme as well as the frequency-shift mechanism will be reported in the near future.

In Sec. II, the spontaneous spectrum of a tapered wiggler is discussed briefly. In Sec. III, an analytical expression of the small-signal gain is derived for an arbitrary wiggler and expressed in terms of the spontaneous spectrum. Different schemes, such as constant wiggler (CW), tapered wiggler (TW), multicomponent wiggler (MCW), and optical klystron (OK) are studied in Sec. IV based on the simple gain expression. In Sec. V, an upper limit is set for the small-signal gain. Its implication is then discussed. The results are summarized in Sec. VI.

II. SPONTANEOUS SPECTRUM

In this section, we calculate the classical radiation due to the periodic electron motion in a tapered wiggler. Earlier calculations on the spontaneous emission for a constant wiggler have been given by Motz[8] and Colson.[9] The wiggler is assumed to have plane polarization and the vector potential can be written as

$$\vec{A}_\perp(z)=A(z)\cos\left[\int_0^z k_w(z)dz\right]\hat{x} . \tag{1}$$

The calculations can be easily generalized to any field polarization. Far away from the wiggler, the energy received at the detector dW, per unit angle $d\Omega$, per unit frequency interval $d\omega$, is[10]

$$\frac{dW}{d\Omega\, d\omega}=\frac{e^2\omega^2}{4\pi^2 c}\left|\int_0^L \hat{n}\times[\hat{n}\times\vec{\beta}(x)]e^{i(\omega/c)\int_0^z[1-\hat{n}\cdot\vec{\beta}(z)]dz}dz\right|^2 , \tag{2}$$

where $\hat{n}$ is the direction of observation, L is the wiggler length, $\vec{\beta}(z)$ is the electron velocity at position z in units of the light velocity in vacuum c, and ω is the emission frequency.

The integral in (2) represents the complex field amplitude and contains all the information of the electron motion inside the wiggler. We are especially interested in the forward spontaneous spectrum where $\hat{n}=\hat{z}$. In this direction, the complex amplitude becomes

$$\begin{aligned} Q&=\int_0^L \beta_\perp(z)e^{i(\omega/c)\int_0^z[1-\beta_z(z)]dz}dz , \\ \beta_\perp(z)&=-\frac{eA(z)}{\gamma mc^2}\cos\left[\int_0^z k_w(z)dz\right] . \end{aligned} \tag{3}$$

In the integrand in (3), $\beta_\perp(z)$ is the electron transverse velocity indicating the radiation strength at position z while

$$\left[\omega/c\int_0^z[1-\beta_z(z)]dz\right]$$

is the relative phase delay of the radiation arriving at the detector. If the longitudinal velocity β_z is a constant (for example, in a constant helical wiggler), the complex amplitude is the Fourier transform of the electron transverse motion. If β_z is not a constant, the situation is more complicated. However, the fast oscillations in β_z can be averaged over to obtain

$$Q=-\frac{1}{2\gamma}\int_0^L a_w(z)e^{-if(z)}dz\ , \tag{4}$$

where

$$f(z)=\int_0^z g(z)dz\ ,$$

$$g(z)=k_w(z)-\frac{k_s}{2\gamma^2}\left[1+\frac{a_w^2(z)}{2}\right]\ ,$$

$$a_w(z)=\frac{eA(z)}{mc^2},\quad k_s=\frac{\omega}{c}\ .$$

$g(z)$ is the local detuning function between the electron and the ponderomotive potential. $f(z)$ is the accumulated phase factor. For given $a_w(z)$ and $k_w(z)$, the spontaneous spectrum can be obtained by calculating the integral in (4). The detailed result for several wiggler schemes is shown in Sec. IV.

III. SMALL-SIGNAL GAIN

The interaction of an electron with the radiation inside the wiggler can be described by the following one-dimensional equations of motion:

$$\frac{d\xi}{dz}=-k_s a_s a_w(x)\sin\psi\ , \tag{5a}$$

$$\frac{d\psi}{dz}=k_w(z)-\frac{k_s}{2\xi}\left[1+\frac{a_w^2(z)}{2}-a_s a_w(z)\cos\psi\right]\ ,$$

$$\psi=\int(k_w+k_s)dz-\omega_s t\ , \tag{5b}$$

$$\xi\equiv\gamma^2\ ,$$

$$a_s\equiv\frac{eE}{k_s mc^2}\ ,$$

where E is the radiation field amplitude, and ψ is the phase position of the electron in the ponderomotive potential well. In Eqs. (5a) and (5b), we have averaged over the fast oscillations of the electron motion at the radiation and wiggler period. The term $(a_s a_w\cos\psi)$ in (5b) is small and usually neglected in the calculation of the gain. However, we find this term is essential in providing an exact relation between the small-signal gain and the spontaneous spectrum as it will be shown later.

In the small-signal regime, the dynamic variables ξ and ψ can be expanded in powers of a_s:

$$\begin{aligned}\xi&=\xi^{(0)}+\xi^{(1)}+\xi^{(2)}+\cdots\ ,\\ \psi&=\psi^{(0)}+\psi^{(1)}+\cdots\ ,\end{aligned} \tag{6}$$

where $\xi^{(n)}$ and $\psi^{(n)}$ represent the terms proportional to a_s^n. Substituting (6) into (5), we have the following iterative equations:

$$\frac{d\psi^{(0)}}{dz}=k_w(z)-\frac{k_s}{2\xi^{(0)}}\left[1+\frac{a_w^2(z)}{2}\right]\ , \tag{7a}$$

$$\frac{d\xi^{(1)}}{dz}=-k_s a_s a_w(z)\sin\psi^{(0)}\ , \tag{7b}$$

$$\frac{d\psi^{(1)}}{dz}=\frac{k_s\xi^{(1)}}{2\xi^{(0)2}}\left[1+\frac{a_w^2(z)}{2}\right]+\frac{k_s a_s a_w(z)}{2\xi^{(0)}}\cos\psi^{(0)}\ , \tag{7c}$$

$$\frac{d\xi^{(2)}}{dz}=-k_s a_s a_w(z)\psi^{(1)}\cos\psi^{(0)}\ ; \tag{7d}$$

with the initial condition $\xi^{(0)}=\gamma^2$, $\xi^{(1)}$ and $\xi^{(2)}$ can be obtained by straightforward integrations of (7):

$$\xi^{(1)}=-k_s a_s\int_0^L a_w(z)\sin[\psi_0+f(z)]dz\ , \tag{8a}$$

$$\xi^{(2)}=-\frac{k_s^2a_s^2}{4\gamma^2}\left[\int_0^L a_w(z)\cos[\psi_0+f(z)]dz\right]^2+\frac{k_s^3a_s^2}{2\gamma^4}\int_0^L a_w(z)\cos[\psi_0+f(z)]dz\int_0^z\left[1+\frac{a_w^2(z')}{2}\right]dz'\times\int_0^{z'}a_w(z'')\sin[\psi_0+f(z'')]dz''\ , \tag{8b}$$

where ψ_0 is the initial phase of the electron and $f(z)$ has been given in (4). We are interested in the electron energy in units of the electron rest mass γ, which is related to the dynamic variable ξ as

$$\gamma^{(1)}=\frac{\xi^{(1)}}{2\gamma}\ , \tag{9a}$$

$$\gamma^{(2)}=\frac{1}{2\gamma}\left[\xi^{(2)}-\frac{\xi^{(1)2}}{4\gamma^2}\right]\ . \tag{9b}$$

Substituting (8) into (9), we obtain the first- and second-order corrections to the electron energy. We can then go on to calculate the ensemble averages (over the initial phase ψ_0) of two quantities: the phase averaged energy change $\langle \Delta\gamma \rangle$ and the phase averaged energy spread $\langle (\Delta\gamma)^2 \rangle$ that are related to the small-signal gain and the spontaneous spectrum, respectively, for small-gain systems and monoenergetic beams. Although this calculation is straightforward, it utilizes a number of algebraic manipulations that are described in detail in Appendix A and yields the following results:

$$\langle (\Delta\gamma)^2 \rangle = \langle \gamma^{(1)^2} \rangle = \frac{k_s^2 a_s^2}{8\gamma^2} \int_0^L dz_1 \int_0^L dz_2 a_w(z_1) a_w(z_2) \cos[f(z_1) - f(z_2)] , \tag{10a}$$

$$\langle \Delta\gamma \rangle = \langle \gamma^{(2)} \rangle = -\frac{k_s^2 a_s^2}{16\gamma^2} \int_0^L dz_1 \int_0^L dz_2 \left[\frac{2}{\gamma} - \frac{\partial}{\partial\gamma} \right] \{ a_w(z_1) a_w(z_2) \cos[f(z_1) - f(z_2)] \} . \tag{10b}$$

Comparing (10b) and (10a), we prove Madey's theorem[11,12]

$$\langle \Delta\gamma \rangle = \frac{1}{2} \frac{\partial}{\partial\gamma} \langle (\Delta\gamma)^2 \rangle . \tag{11}$$

It has to be emphasized that we have proved this theorem for any wiggler configuration. Further, the wiggler variation does not need to be symmetric as the assumption given in the original paper.[11] Since there is essentially no restrictions on $a_w(z)$ and $k_w(z)$, the theorem is also applicable to the multicomponent wiggler or the optical klystron as long as $a_w(z)$ and $k_w(z)$ are slowly varying.

The small-signal gain in the radiation power $\mathscr{E} = cE^2/8\pi$ can be derived from the extraction efficiency η, if it is assumed that all the energy lost by the electron beam goes into electromagnetic energy:

$$\eta \equiv -\frac{\langle \Delta\gamma \rangle}{\gamma} = -\frac{k_s^2 a_s^2}{\gamma} \frac{\partial}{\partial\gamma} |Q|^2 , \tag{12}$$

$$G \equiv \frac{\mathscr{E}(L) - \mathscr{E}(0)}{\mathscr{E}(0)} = \eta \frac{\mathscr{I}_{e\,\text{beam}}}{\mathscr{I}_{\text{radiation}}} = -\frac{\omega_p^2}{2c^2} \frac{\partial}{\partial\gamma} |Q|^2 , \tag{13}$$

where $\mathscr{I}$ represents input power and $|Q|^2$ was given in (4). From (9), we find that the small-signal gain is exactly proportional to the slope of the spontaneous spectrum. Note that if the small term in (5b) would have been neglected, the small-signal gain would be

$$G' = -\frac{\omega_p^2}{2c^2} \left[\frac{\partial}{\partial\gamma} + \frac{2}{\gamma} \right] |Q|^2 . \tag{14}$$

Although $(2/\gamma)$ is much smaller than $(\partial/\partial\gamma)$ in the relativistic limit, it violates the exact relation that follows from Madey's theorem.

The gain expression in (13) is completely general. It is derived for arbitrary variation in the magnetic amplitude and period including multicomponent devices and optical klystrons. In these devices, the drift space can be represented by $a_w(z) = k_w(z) = 0$. As will be shown in Sec. IV, an optical klystron is a particular case of the multicomponent device. Instead of its physical drift distance, we have to apply the effective drift distance which is due to the use of dispersion magnets.

IV. APPLICATIONS

In this section the formulas derived in Secs. II and III for the spontaneous spectrum and small-signal gain are applied to particular devices. We first show that for a constant wiggler the standard result is obtained and afterwards generalized to a tapered wiggler and a multicomponent wiggler.

A. Constant wiggler

For a constant wiggler, the complex field amplitude is reduced to

$$Q_c = \frac{a_w}{2\gamma} \int_0^L e^{-ihz} dz , \qquad h = k_w - \frac{k_s}{2\gamma^2} \left[1 + \frac{a_w^2}{2} \right] . \tag{15}$$

Hence, its spontaneous spectrum is the well-known spherical Bessel function squared

$$\frac{dW}{d\Omega\, d\omega} = \frac{e^2 \omega^2 a_w^2 L^2}{16\pi^2 c\gamma^2} j_0^2(x) \Big|_{x = hL/2} . \tag{16}$$

The small-signal gain, obtained as shown in Eq. (13), is

$$G_c=\frac{\omega_p^2 k_w L^3 a_w^2}{2c^2\gamma^3}\frac{2-2\cos x-x\sin x}{x^3}\bigg|_{x=hL}, \tag{17}$$

and it peaks at $hL=2.6$, yielding the standard formula

$$G_{c,\max}=0.27\frac{\omega_p^2 k_w L^3 a_w^2}{4c^2\gamma^3}. \tag{18}$$

B. Linearly tapered wiggler

For a tapered wiggler with the variations $a_w(z)$ and/or $k_w(z)$, Eqs. (4) and (13) can be used to calculate the gain and the spontaneous spectrum numerically. Since the spectrum is the result of interference of the fields radiated from different parts of the wiggler, the phase factor $f(z)$ is far more important and sensitive than the radiative strength factor $a_w(z)$. For simplicity, we consider the linearly tapered wiggler with the variation

$$g(z)=h+\alpha z \tag{19}$$

and calculate the spontaneous spectrum to be

$$\frac{dW}{d\Omega\, d\omega}=\frac{e^2\omega^2 a_w^2}{16\pi^2 c\gamma^2}\frac{\pi}{\alpha}\{[C(p)-C(q)]^2+[S(p)-S(q)]^2\},$$

$$p=\left[\frac{\alpha}{\pi}\right]^{1/2}L+\frac{h}{\sqrt{\alpha\pi}}, \tag{20}$$

$$q=\frac{h}{\sqrt{\alpha\pi}},$$

where h is the initial energy detuning, α indicates the degree of linear tapering, C and S are Fresnel functions.[13] Since

$$C(-p)=-C(p);\quad S(-p)=-S(p), \tag{21}$$

the spectrum is symmetric about $p=-q$, i.e.,

$$h=-\alpha L/2, \tag{22}$$

which means that the wavelength at which the spectrum is centered is determined by the parameters at the mid wiggler. If we choose to fix the wiggler parameters at the entrance, as we vary the wiggler taper, it is expected that the center of the spectrum will shift to lower values of h (shorter wavelengths for a fixed electron energy) with increasing tapering for positive α. The spectrum, for values of $\alpha L^2=0,10,20,30,40,50$ is shown in Fig. 1. When the taper increases, we find that the peak intensity drops while the first sideband is enhanced. In particular, at $\alpha L^2=30$, the magnitudes of the fundamental and first sideband are almost the same and the spectrum shows a plateau extending over a wide range. For αL^2 larger than 30, the center intensity drops even further and the spectrum extends rather irregularly.

It is useful to relate the parameter α to the taper rate for constant amplitude or constant period wigglers. For constant amplitude

$$\alpha=\frac{k_w}{L}\frac{\lambda_w(0)-\lambda_w(L)}{\lambda_w(0)}, \tag{23}$$

and for constant period

$$\alpha=\frac{a_w^2}{1+a_w^2/2}\frac{k_w}{L}\frac{a_w(0)-a_w(L)}{a_w(0)}. \tag{24}$$

In the TRW 10.6-μm experiment, a 3% tapering in a_w gives $\alpha L^2=10$.

The small-signal gain for a linearly tapered wiggler is obtained by taking the derivative of (20):

$$G=\frac{\omega_p^2 a_w^2 k_w\sqrt{\pi}}{2c^2\gamma^3\alpha\sqrt{\alpha}}\left[\left[\cos\frac{\pi p^2}{2}-\cos\frac{\pi q^2}{2}\right][C(p)-C(q)]+\left[\sin\frac{\pi p^2}{2}-\sin\frac{\pi q^2}{2}\right][S(p)-S(q)]\right], \tag{25}$$

which is identical to the result obtained by Brau.[14] The gain spectrum is antisymmetric about the point $p=-q$ and is shown in Fig. 2 as a function of the wiggler taper and the energy detuning. To simplify the figure, the negative gains are suppressed; however, they can be figured out easily from the antisymmetry relation. Figure 2 shows that the main bump in the spectrum decreases appreciably and disappears completely after $\alpha L^2=30$. The small bumps on the negative side of h vanish even faster except for a rising bump within the range $-2\pi<(hL+\alpha L^2/2)<0$. This becomes the major contribution at large tapering. It is interesting to note that the peak gains shift toward negative h and decrease in magnitude as the taper rate increases. Eventually, the first side lobe disappears completely and is replaced by the main peak, as the shift of the whole structure continues, the relative amplitude between the main peak and the remaining sidebands decreases and can become smaller than one. Thus, the spectrum tends to remain rich in structure and with its maximum gain near $h\simeq 0$ ($\gamma\simeq\gamma_R$). In or-

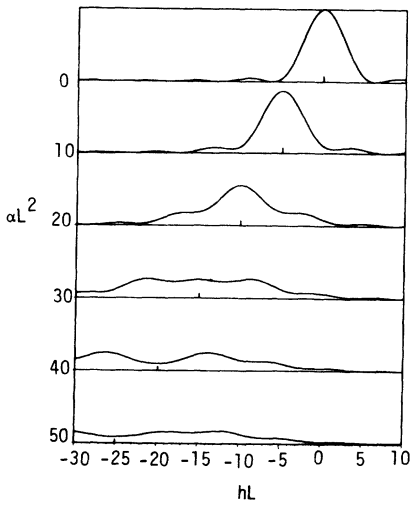

FIG. 1. Spontaneous spectra at different wiggler tapers.

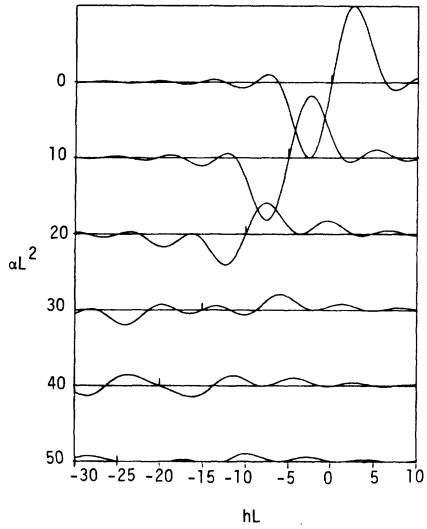

FIG. 3. Gain spectra at different wiggler tapers.

der to compare with Fig. 1, the gain spectrum is shown explicitly in Fig. 3 for the corresponding linear taperings.

In Fig. 4, the relative value of the gain is shown in contours of equal gain. The value indicated on each curve is the gain compared to the maximum gain (0.27) for the constant wiggler [see Eq. (18)]. Note that, at $\gamma=\gamma_R$, the gain can be negative for certain tapering ranges. Obviously, for the oscillator startup at the desired wavelength, these regions should be avoided.

C. Two-component wiggler and optical klystron

A two-component wiggler device is composed of two wigglers (constant[2] or tapered[3,4]) in series with a free-drift space between them [Fig. 5(a)]. For a first component or prebuncher of appropriate length, the electron bunching usually increases with the drift distance. In order to increase the drift distance without affecting the device length, dispersion magnets are introduced in the drift space. A typical arrangement is shown in Fig. 5(b). The free-drift space can be represented by $a_w=k_w=0$. The phase advance of the electron relative to the radiation in the free-drift space can be calculated from the phase equation. With a drift distance L_D, the phase change is

$$\psi=-\frac{k_s}{2\gamma^2}L_D\ . \tag{26}$$

For two electrons with energy difference $\Delta\gamma$, the difference in the phase change is

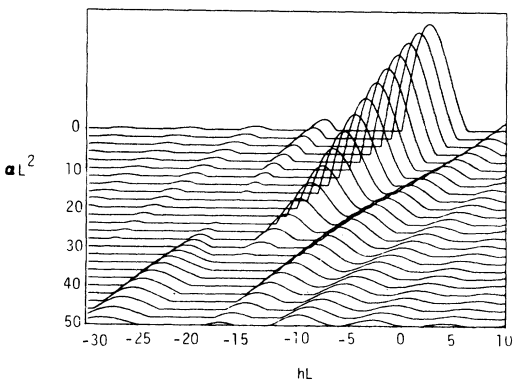

FIG. 2. Gain structure as a function of the taper αL^2 and the detuning parameter hL. The negative gains are suppressed.

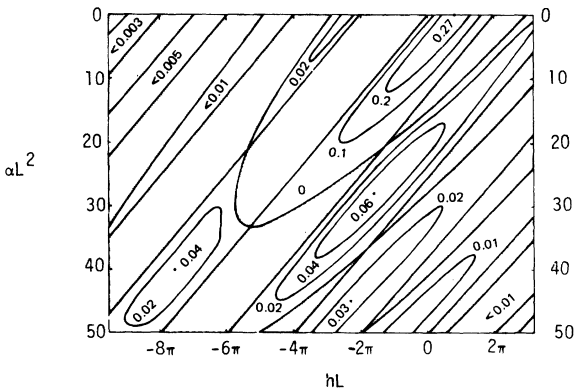

FIG. 4. Value of gain shown in contours. The value indicated on each curve is the gain compared to the maximum gain of a constant wiggler (0.27).

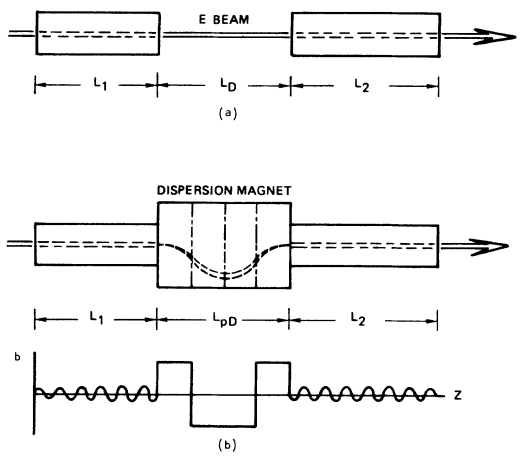

FIG. 5. Typical geometry of a two-component wiggler (a) and an optical klystron (b). The lowest curve shows the wiggler field and the dispersion magnetic field in the drift space.

$$\Delta\psi=\frac{k_s L_D}{\gamma^3}\Delta\gamma\ . \tag{27}$$

For the dispersion magnets, the electron flight time is highly energy dependent. For the dispersion magnetic field geometry shown in Fig. 5(b), the induced phase difference for $\Delta\gamma$ is found to be

$$\Delta\psi=\frac{k_s L_{pD}^3}{48\gamma^3}\left[\frac{eB}{mc^2}\right]^2\Delta\gamma\ . \tag{28}$$

Comparing (28) with (27), we conclude that an optical klystron with a dispersion magnet is equivalent to a two-component device with an effective drift distance

$$L_D=\frac{L_{pD}^3}{48}\left[\frac{eB}{mc^2}\right]^2\ . \tag{29}$$

The effective drift distance is proportional to the magnetic field squared and to the cube of the physical distance between two sections L_{pD}. Since these two devices are equivalent, both can be described by calculating the gain for a two-component device with an effective drift distance L_D. In order to calculate the small-signal gain we first have to evaluate the integral Q in the spontaneous spectrum.

Since $|Q|^2$ is a double integral of real functions,

$$|Q|^2=\frac{1}{4\gamma^2}\int_0^L dz_1\int_0^L dz_2 a_w(z_1)a_w(z_2)\cos[f(z_1)-f(z_2)]\ , \tag{30}$$

the integration can be divided into three regions: (i) $0\le(z_1,z_2)\le L_1$; (ii) $L_1+L_D\le(z_1,z_2)\le L$; (iii) $0\le z_1\le L_1, L_1+L_D\le z_2\le L$ or $0\le z_2\le L_1, L_1+L_D\le z_1\le L$. The integral in the first region represents the spontaneous spectrum from the first wiggler while the integral in (ii) represents the radiation from the second wiggler. The integral in region (iii) represents the interference of the radiation fields radiated from different wigglers. Therefore

$$|Q|^2=|Q_1|^2+|Q_2|^2+\frac{1}{2\gamma^2}\int_0^{L_1}dz_1\int_0^{L_2}dz_2 a_{w1}(z_1)a_{w2}(z_2)\cos\times\left[f_1(L_1)-f_1(z_1)+f_2(z_2)-\frac{k_s}{2\gamma^2}L_D\right]\ , \tag{31}$$

where $|Q_1|^2$ and $|Q_2|^2$ are the terms corresponding to the spontaneous emission from individual sections without mutual interference. From (31), we observe that the spontaneous spectrum, in general, is not the same when we exchange the position of two wigglers unless the whole device is symmetric, i.e., $L_1=L_2$ and

$$\begin{aligned} a_{w1}(L_1-z)&=a_{w2}(z)\ ,\\ g_1(L_1-z)&=g_2(z)\ , \end{aligned} \tag{32}$$

where $g(z)$ is the local detuning parameter defined in (4). The small-signal gain, which is the derivative of $|Q|^2$, is thus not the same for both cases.

In what follows, we will analyze two two-component wiggler devices: constant-constant wiggler (CCW) and constant-tapered wiggler (CTW). CCW is the usual case considered in optical klystrons while CTW is suggested for the enhancement of the small-signal gain of TWFEL. For the case of CCW with the same constant parameters a_w and k_w, $|Q|$ is calculated to be

$$|Q|^2=\frac{a_w^2}{2h^2\gamma^2}\left\{1-\tfrac{1}{2}\cos hL_1-\tfrac{1}{2}\cos hL_2+2\sin\frac{hL_1}{2}\sin\frac{hL_2}{2}\cos\left[\tfrac{1}{2}\left[hL_1+hL_2-\frac{k_sL_D}{\gamma^2}\right]\right]\right\}. \tag{33}$$

The small-signal gain is obtained by taking the derivative of (33) with respect to γ. In the case of an optical klystron with dispersion magnets, L_D is much larger than L_1 or L_2, and we have

$$\frac{\partial|Q|^2}{\partial\gamma}=-\frac{a_w^2k_sL_D}{h^2\gamma^5}\sin\frac{hL_1}{2}\sin\frac{hL_2}{2}\sin\left[\tfrac{1}{2}\left[h(L_1+L_2)-\frac{k_sL_D}{\gamma^2}\right]\right]. \tag{34}$$

The values of hL_1 and hL_2 are of the order of unity. The quantity $(k_sL_D/2\gamma^2)$ can be varied within a range of 2π by just changing L_D within a magnetic period. Therefore, we can always adjust L_D such that the third sine function becomes one. The function $(\sin hL_1/2\sinh L_2/2)$ is maximum when $L_1=L_2=L_0$. Therefore, for the same total interaction length, we get the best efficiency when the two sections are identical. The maximum gain for an optical klystron with dispersion magnets is obtained at $h=0$:

$$G_{\max}^{\mathrm{OK}}=\frac{a_w^2\omega_p^2\omega L_0^2L_D}{2c^3\gamma^5}. \tag{35}$$

Comparing this gain to the maximum gain of a constant wiggler of length $2L_0$, we find

$$\frac{G_{c,\max}^{\mathrm{OK}}}{G_{c,\max}}=\frac{1}{0.54(1+a_w^2/2)}\frac{L_D}{L_0} \tag{36}$$

which shows the factor of gain enhancement by an optical klystron. The result is in agreement with previous derivations.[2] From (35), we find that the maximum gain is proportional to the interaction length squared L_0^2, and the effective drift distance L_D. The width of the gain spectrum can be found from (34):

$$\Delta\left[\frac{k_sL_D}{2\gamma^2}\right]=\pi$$

or

$$\frac{\Delta\lambda_s}{\lambda_s}=\gamma^2\frac{\lambda_s}{L_D}. \tag{37}$$

When L_D is large, the value in (37) is very small and highly restricts the electron energy spread to avoid a decrease in gain. For example, for $\lambda_s=10$ μm, $L_D=10m$ and $\gamma=50$; the electron energy spread is required to be less than 0.25%.

One has to be reminded that the introduction of L_D has two purposes. It transforms the energy modulation of the beam from the first wiggler into space modulation and places the modulated beam at the best phase position for the energy extraction in the second wiggler. The space modulation process needs a length comparable to or longer than the interaction length and is responsible for the high maximum gain in (35). The phase adjustment requires a much shorter distance of the order of the magnetic period; it appears in the argument of the last sine function in (34). These two characteristic distances are so different in their orders of magnitude that they can be taken as independent parameters.

Next, we consider a two-component device where one of the wigglers is linearly tapered. The constant section can be put in front of the tapered section (constant-tapered wiggler, CTW) or after the tapered section (tapered-constant wiggler, TCW). Both schemes can be used to enhance the small-signal gain over that of a tapered wiggler of the same total length. CTW is also especially useful at large signals because the constant section provides a bunched electron beam for the tapered section. By substituting the function $f(z)$ for both sections into (31), we can calculate the interference term in $|Q|^2$. The details of this calculation are presented in Appendix B:

$$|Q|^2_{\mathrm{interf}}=\left[\frac{\pi}{\alpha}\right]^{1/2}\frac{a_{wc}a_{wt}}{h_c\gamma^2}\sin\frac{h_cL_c}{2}\{\cos M[C(p)-C(q)]+\sin M[S(p)-S(q)]\}, \tag{38}$$

where α, p, and q are given in (20) in terms of the parameters of the tapered section. The subscripts c and t indicate the quantity for constant and tapered sections, respectively, and

$$M=\begin{cases}\dfrac{h_t^2}{2\alpha}+\dfrac{k_sL_D}{2\gamma^2}-\dfrac{h_cL_c}{2} & \text{for CTW}\\[2ex] \dfrac{(\alpha L_t+h_t)^2}{2\alpha}-\dfrac{k_sL_D}{2\gamma^2}+\dfrac{h_cL_c}{2} & \text{for TCW}\end{cases} \tag{39}$$

where h_c and h_t are the degrees of detuning for the CW and TW, respectively. Therefore, both schemes produce similar spectrums except for the argument M.

If L_D is much larger than L_c or L_t (which is the case if a dispersion magnet is used) the gain can be obtained easily by taking the derivatives of $\sin M$ and $\cos M$ in Eq. (38) and all terms except those proportional to L_D can be discarded. In that case

$$G=\pm\left[\frac{\pi}{\alpha}\right]^{1/2}\frac{\omega_p^2 a_{wc}a_{wt}k_w L_D}{c^2\gamma^3 h_c}\sin\frac{h_c L_c}{2}\{\sin M[C(p)-C(q)]-\cos M[S(p)-S(q)]\}\ , \tag{40}$$

where positive and negative signs are for CTW and TCW, respectively. The gain becomes maximum at $h_c=0$. If h_t is also chosen to be zero and αL^2 is a large number, we have $C(p)\approx S(p)\approx\frac{1}{2}$ and $C(q)=S(q)=0$. The functions $\sin M$ and $\cos M$ are fast oscillating as L_D varies. The value in the curly brackets in (40) can be maximized by adjusting the drift distance within a magnetic period. Choosing $h_c=0$ and $M=(n+\frac{1}{4})\pi$, the maximum gain for both schemes becomes

$$G=\frac{\omega_p^2 a_{wc}a_{wt}L_c L_D k_w}{2c^2\gamma^3}\left[\frac{\pi}{2\alpha_t}\right]^{1/2}. \tag{41}$$

Note that the length of the taper enters in the gain expression through α_t. From (25), we find that the maximum small-signal gain for a tapered wiggler of length (L_c+L_t) is

$$G_{\max}^T=\frac{(\sqrt{2}-1)\omega_p^2 a_w^2 k_w}{2c^2\gamma^3}\left[\frac{\pi}{\alpha_{ct}^3}\right]^{1/2}. \tag{42}$$

To simplify the comparison between (41) and (42), we assume that $a_{wc}=a_{wt}(0)=a_w(0)$ and $a_{wt}(L_t)=a_w(L_c+L_t)$, i.e., both tapered wigglers have the same percentage change in a_w or $\alpha_t L_t^2=\alpha_{ct}(L_c+L_t)^2$. The gain-enhancement factor is then obtained by taking the ratio of (41) and (42):

$$\frac{G}{G_{\max}^T}=\frac{k_w L_c L_D a_w^2\delta}{(2-\sqrt{2})\mu^2(L_c+L_t)}\left[\frac{L_t}{L_c+L_t}\right]^{1/2}, \tag{43}$$

where δ is the percentage change in a_w for both tapered wigglers. For example, if we have $L_c=L_t$ and $a_w=1$, the enhancement factor becomes

$$\frac{G}{G_{\max}^T}\cong 2.5\delta\frac{L_D}{\lambda_w}\ . \tag{44}$$

Thus, the enhancement could be orders of magnitude large.

In order to simplify the analytical expression, we have calculated the small-signal gain enhancement of a tapered wiggler by using dispersion magnets, with $L_D\gg L_c, L_t$. However, if an enhancement of gain by about ten times is sufficient for our purpose, we find that a two-component device *without* drift space is good enough. For example, if the small-signal gain of a 3-m long tapered wiggler is to be enhanced, it can be broken into a 1-m constant section and a 2-m tapered section with the same percentage change in a_w. We keep a small gap between the two sections. The gap, which is about the distance of a magnetic period, works as a phase adjustor such that the modulated electron beam that comes out of the constant section can be placed at the optimum phase for the energy extraction in the tapered section at large signals. Numerically, we find that the gain can be enhanced by five to ten times without reducing the gain in the large-signal regime.[4] In this case, the small-signal gain is, in general, determined by the constant wiggler section small-signal gain which is well above the threshold value for a FEL oscillator.

V. MAXIMUM GAIN

The gain expression has been obtained in a double integration of real functions

$$G=\frac{\omega_p^2\omega_w}{4\gamma^3 c^3}\int_0^L dz_1\int_0^L dz_2 a_w(z_1)a_w(z_2)(z_1-z_2)\sin[f(z_1)-f(z_2)]\ , \tag{45}$$

where for the purpose of this discussion we have neglected the term $(2/\gamma)$ compared to $(\partial/\partial\gamma)$. From (45), an upper bound for the small-signal gain can be set easily because the absolute value of a sine function cannot be larger than one:

$$G \leq G_{\text{limit}} = \frac{\omega_p^2 \omega_w}{4\gamma^3 c^3} \int_0^L dz_1 \int_0^L dz_2 a_{w,\max}^2 \, | z_1 - z_2 |$$
$$= \frac{\omega_p^2 \omega_w}{4\gamma^3 c^3} \frac{a_{w,\max}^2 L^3}{3} , \tag{46}$$

where $a_{w,\max}$ is the maximum value of $a_w(z)$. Comparing (46) to (18), it is found that the upper limit for the small-signal gain can exceed the maximum gain for a constant wiggler only by less than 25% if no dispersion magnets are used. An interesting question is the following: Within this small margin is there any other wiggler variation which can give a higher gain than the maximum gain of a constant wiggler with the same total length?

This question can be answered by using an approach similar to the calculus of variation. For simplicity, we consider that a small perturbing variation is introduced to the phase factor but not to the radiation strength of the constant wiggler

$$f(z) = hz + \delta\eta(z); \quad a_w = \text{const} , \tag{47}$$

where δ is an arbitrarily small number so that results can be expanded in powers of δ, and $\eta(z)$ is an arbitrary function. After substituting (47) into (42), the gain can be expanded in power series of δ. If there is no other variation which can give a higher gain than the maximum gain of the constant wiggler, the following condition must be satisfied for any function $\eta(z)$:

$$\left. \frac{\partial G}{\partial \delta} \right|_{hL=2.6;\delta=0} \equiv 0 . \tag{48}$$

This identity requires the following function to be zero:

$$J = \int_0^L dz_1 \int_0^L dz_2 (z_1 - z_2)[\eta(z_1) - \eta(z_2)]\cos[h(z_1 - z_2)]$$
$$= 2 \int_0^L dz_1 \eta(z_1) \int_0^L dz_2 (z_1 - z_2)\cos[h(z_1 - z_2)] . \tag{49}$$

Since $\eta(z)$ is arbitrary, it can be chosen to be a set of orthogonal functions in the interval $[0,L]$ for example, $\eta(z)$ can be the Legendre functions if the integration range is properly transformed into $[-1,1]$. From the completeness of orthogonal functions, the following integral has to vanish for any value of z_1:

$$\int_0^L dz_2 (z_1 - z_2)\cos[h(z_1 - z_2)] = 0 . \tag{50}$$

It is straightforward to check that (50) cannot be satisfied. Therefore, the conclusion is that the constant-wiggler gain is not the maximum gain that can be obtained. By properly recontouring the wiggler variation, we expect that the gain can be increased although the proof does not show a best way to change the tapering. It is interesting to point out that the linear taper given in (19) does satisfy the condition (48). However, if the perturbing function $\eta(z)$ is chosen to be cubic, the condition (45) is not satisfied and we obtain a gain higher than (18). The increase in the gain is obviously due to the generation of complex structures in the spontaneous spectrum. The change in its slope cannot be very big and thus the increase in gain is very limited.

The analysis can be generalized to the perturbation on any given wiggler variation. For example, consider a wiggler with the variation $f(z)$. Following a similar procedure, we can prove that the gain for that wiggler is a maximum only when

$$\int_0^L dz_2 (z_1 - z_2)\cos[f(z_1) - f(z_2)] = 0 \tag{51}$$

for any value of z_1. Again, it is straightforward to show that (48) cannot be satisfied for any variation $f(z)$. Therefore, a generalized conclusion is that for any wiggler configuration, another configuration can be found that produces a higher gain within the 25% margin. Thus, the gain can always be increased, within the 25% margin, over the maximum constant-wiggler gain, by properly changing the tapering.

The results presented in the previous sections were spot checked numerically with a 1D particle simulation code that includes electron beam energy spread, finite emittance, and a Gaussian diffraction of the total radiation power.[4] Although some of the structure of the small-signal gain was smoothed out, it was found that the numerical results were in agreement with the analytical predictions for the maximum small-signal gain within 10 to 20% for

parameters similar to those of the present TRW experiment.[15] The details of these simulations will be published in the near future.[16]

VI. SUMMARY

We have completed a small-signal theory for an arbitrary FEL wiggler. The spontaneous spectrum and the small-signal gain are derived analytically for a cold electron beam and a plane input wave. Madey's theorem is then proved for the most general wiggler configuration. The gain expression is applied to special cases such as constant wiggler, linear tapered wiggler, two-component devices, and optical klystron. An upper limit is found for the small-signal gain of any wiggler configuration which can exceed the maximum gain of a constant wiggler of the same length by less than 25%. The significance of its implication is discussed. For an optical klystron with dispersion magnets, it is found that the upper limit is determined from the equivalent device length which is much higher than the value determined from its physical length. The gain is thus possible to be highly enhanced with dispersion magnets in the drift space. In addition, for a tapered wiggler, it is found that the small-signal gain can be enhanced even without dispersion magnets or drift space by exchanging part of the tapered wiggler by a constant-wiggler magnet.[3]

ACKNOWLEDGMENTS

The authors would like to acknowledge useful discussions with Dr. H. Boehmer, Dr. J. Edighoffer, Dr. S. Fornaca, Dr. J. Munch, Dr. G. Neil, and Dr. B. Saur. This work was supported by the AFOSR Contract No. F49620-80-C-0079.

APPENDIX A

In this appendix, we show the derivation of $\langle(\Delta\gamma)^2\rangle$ and $\langle\Delta\gamma\rangle$ in detail. From (8a), we have

$$\xi^{(1)^2}=k_s^2a_s^2\left[\int_0^L a_w(z)\sin[\psi_0+f(z)]dz\right]^2$$
$$=k_s^2a_s^2\int_0^L dz_1\int_0^L dz_2 a_w(z_1)a_w(z_2)\sin[\psi_0+f(z_1)]\sin[\psi_0+f(z_2)]\ ; \tag{A1}$$

the phase average of (A1) gives

$$\langle\xi^{(1)^2}\rangle=\frac{k_s^2a_s^2}{2}\int_0^L dz_1\int_0^L dz_2 a_w(z_1)a_w(z_2)\cos[f(z_1)-f(z_2)]\ . \tag{A2}$$

By substituting (A2) into (9a), we obtain the result in (10a). To calculate $\langle\Delta\gamma\rangle$, we use the relation (9b)

$$\gamma^{(2)}=\frac{1}{2\gamma}\left[\xi^{(2)}-\gamma^{(1)^2}\right]\ . \tag{A3}$$

Equation (8b) shows that $\xi^{(2)}$ consists of two terms

$$\xi^{(2)}=\xi_a^{(2)}+\xi_b^{(2)}\ , \tag{A4}$$

where $\xi_a^{(2)}$ is the square of an integral while $\xi_b^{(2)}$ is a triple integration. $\xi_a^{(2)}$ is very similar to $\xi^{(1)^2}$. Actually, following the same procedures in (A1) and (A2), we find

$$\langle\xi_a^{(2)}\rangle=-\langle\gamma^{(1)^2}\rangle\ . \tag{A5}$$

To simplify the calculation of $\langle\xi_b^{(2)}\rangle$, we rearrange the order of the integrations for the last two integrals:

$$\int_0^z dz'\int_0^{z'} dz''\equiv\int_0^z dz''\int_{z''}^z dz'\ , \tag{A6}$$

and $\xi_b^{(2)}$ becomes

$$\xi_b^{(2)}=\frac{k_s^3a_s^2}{2\gamma^4}\int_0^L a_w(z)\cos[\psi_0+f(z)]dz\int_0^z a_w(z'')\sin[\psi_0+f(z'')]dz''\int_{z''}^z\left[1+\frac{a_w^2(z')}{2}\right]dz'\ . \tag{A7}$$

By taking the phase average of (A7) and noting that

$$\int_{z''}^{z}\left[1+\frac{a_w^2(z')}{2}\right]dz'=\frac{\gamma^3}{k_s}\frac{\partial}{\partial\gamma}[f(z)-f(z'')] \tag{A8}$$

we get

$$\langle\xi_b^{(2)}\rangle=\frac{k_s^2a_s^2}{4\gamma}\int_0^L dz\int_0^z dz''a_w(z)a_w(z'')\sin[f(z'')-f(z)]\frac{\partial}{\partial\gamma}[f(z)-f(z'')]\ . \tag{A9}$$

Since the integrand of the double integral in (A9) is symmetric in z and z'', the range of integration can be extended to $\int_0^L dz\int_0^L dz''$. The result is

$$\langle\xi_b^{(2)}\rangle=\frac{k_s^2a_s^2}{8\gamma}\int_0^L dz_1\int_0^L dz_2a_w(z_1)a_w(z_2)\frac{\partial}{\partial\gamma}\{\cos[f(z_1)-f(z_2)]\}\ . \tag{A10}$$

By substituting (A10) and (A2) into (A3), we obtain exactly the result shown in (10b).

APPENDIX B

In this appendix, we calculate the interference part of the spontaneous emission for a constant-tapered wiggler (CTW) or a tapered-constant wiggler (TCW).

For a CTW, the phase functions are

$$\begin{aligned}&f_1(z_1)=h_cz_1\ ,\\&f_2(z_2)=h_tz_2+\frac{\alpha}{2}z_2^2\ .\end{aligned} \tag{B1}$$

The integrand in the double integral (31) becomes

$$\cos\left[f_1(L_1)-f_1(z_1)+f_2(z_2)-\frac{k_s}{2\gamma^2}L_D\right]=\cos\left[h_cL_c-h_cz_1+h_tz_2+\frac{\alpha}{2}z_2^2-\frac{k_s}{2\gamma^2}L_D\right]\ . \tag{B2}$$

The integration over z_1 can be easily calculated and we have

$$|Q|^2_{\text{interf}}=\frac{a_{wc}a_{wt}}{2\gamma^2h_c}\int_0^{L_t}dz_2\left[\sin\left[h_cL_c+h_tz_2+\frac{\alpha}{2}z_2^2-\frac{k_s}{2\gamma^2}L_D\right]-\sin\left[h_tz_2+\frac{\alpha}{2}z_2^2-\frac{k_s}{2\gamma^2}L_D\right]\right] \tag{B3}$$

$$=\frac{a_{wc}a_{wt}}{\gamma^2h_c}\int_0^{L_t}dz_2\sin\frac{h_cL_c}{2}\cos\left[\frac{h_cL_c}{2}-\frac{k_sL_D}{2\gamma^2}+h_tz_2+\frac{\alpha}{2}z_2^2\right]\ . \tag{B4}$$

The result in (38) and (39) follows when the integration in (B4) is carried out and expressed in terms of the Fresnel functions.

For a TCW, the phase functions are

$$\begin{aligned}&f_1(z_1)=h_tz_1+\frac{\alpha}{2}z_1^2\ ,\\&f_2(z_2)=h_cz_2\ .\end{aligned} \tag{B5}$$

The integrand in (31) becomes

$$\cos\left[f_1(L_1)-f_1(z_1)+f_2(z_2)-\frac{k_s}{2\gamma^2}L_D\right]=\cos\left[h_tL_t+\frac{\alpha}{2}L_t^2-h_tz_1-\frac{\alpha}{2}z_1^2+h_cz_2-\frac{k_s}{2\gamma^2}L_D\right]\ . \tag{B6}$$

The integration over z_2 results in

$$|Q|^2_{\text{interf}}=\frac{a_{wc}a_{wt}}{2\gamma^2 h_c}\int_0^{L_t}dz_1\left[\sin\left[h_tL_t+\frac{\alpha}{2}L_t^2-h_tz_1-\frac{\alpha}{2}z_1^2+h_cL_c-\frac{k_s}{2\gamma^2}L_D\right]\right.$$
$$\left.-\sin\left[h_tL_t+\frac{\alpha}{2}L_t^2-h_tz_1-\frac{\alpha}{2}z_1^2-\frac{k_s}{2\gamma^2}L_D\right]\right] \tag{B7}$$

$$=\frac{a_{wc}a_{wt}}{\gamma^2 h_c}\int_0^{L_t}dz_1\sin\frac{h_cL_c}{2}\cos\left[\frac{h_cL_c}{2}-\frac{k_s}{2\gamma^2}L_D+h_tL_t+\frac{\alpha}{2}L_t^2-h_tz_1-\frac{\alpha}{2}z_1^2\right]. \tag{B8}$$

Again, the integration over z gives the result in (38) in terms of the Fresnel functions with different constant M.

[1]N. R. Kroll, P. L. Morton, and M. N. Rosenbluth, in *Physics of Quantum Electronics,* Vol. 7, edited by S. F. Jacobs, H. S. Pilloff, M. Sargent III, M. O. Scully, and R. Spitzer (Addison-Wesley, Reading, Mass., 1980).

[2]C. Shih and A. Yariv, Opt. Lett. 5, 76 (1980).

[3]M. Z. Caponi and C. Shih, *IEEE International Conference on Plasma Science, Santa Fe, New Mexico, 1981* (IEEE, Santa Fe, N.M., 1981); Bull. Am. Phys. Soc. 26, 919 (1981).

[4]The possibility of high signal-gain enhancement with the multicomponent wiggler was suggested first to us by our colleague J. Edighoffer. Also cf M. Z. Caponi and C. Shih, Bull. Am. Phys. Soc. 26, 919 (1981).

[5]V. Stango, G. Brautti, T. Clauser, and T. Boscolo, Nuovo Cimento 56B, 219 (1980).

[6]J. Boscolo and V. Stango, Nuovo Cimento 58B, 267 (1980).

[7]W. B. Colson, *Physics of Quantum Electronics,* Vol. 8, edited by S. F. Jacobs *et al.* (Addison-Wesley, Reading, Mass., 1982).

[8]H. Motz, J. Appl. Phys. 22, 527 (1981).

[9]W. B. Colson, Ph.D. thesis, Stanford University, 1977 (unpublished).

[10]J. D. Jackson, *Classical Electrodynamics* (Wiley, New York, 1976).

[11]J. M. J. Madey, Nuovo Cimento 50B, 64 (1979).

[12]N. M. Kroll, P. L. Morton, and M. N. Rosenbluth, IEEE J. Quantum Electron. RE-17, 1436 (1981).

[13]W. Gautschi, *Handbook of Mathematical Functions,* 9th ed., edited by M. Abramowitz and I. A. Segun (Dover, New York, 1970), Chap. 7.

[14]C. A. Brau, IEEE J. Quantum Electron. 16, 335 (1980).

[15]H. Boehmer, M. Z. Caponi, J. Edighoffer, S. Fornaca, J. Munch, G. R. Neil, B. Saur, and C. Shih, Phys. Rev. Lett., 48, 141 (1982).

[16]M. Z. Caponi and C. Shih (unpublished).